Applied Energy 225 (2018) 392–401

Contents lists available at ScienceDirect

Applied Energy

journal homepage: www.elsevier.com/locate/apenergy

Pilot testing of enhanced sorbents for calcium looping with cement production

María Erans[a], Michal Jeremias[a], Liya Zheng[b,*], Joseph G. Yao[b], John Blamey[b], Vasilije Manovic[a], Paul S. Fennell[b,c], Edward J. Anthony[a,*]

[a] Combustion and CCS Centre, Cranfield University, Bedford, Bedfordshire MK43 0AL, UK
[b] Department of Chemical Engineering, Imperial College London, SW7 2AZ, UK
[c] School of Chemical and Biomolecular Engineering, The University of Sydney, Sydney, NSW 2008, Australia

HIGHLIGHTS

- HBr doping technique for improving calcium looping performance has been demonstrated at pilot scale.
- Attrition resistance of calcium sorbent at pilot scale has been demonstrated due to HBr doping.
- Successful production of cement from the residues has been demonstrated at the kg scale.

ARTICLE INFO

Keywords:
Calcium looping
CCS
Pilot plant
Cement

ABSTRACT

One of the main challenges for commercialising calcium looping (CaL) as a CO_2 capture technology is maintaining a high level of sorbent reactivity during long-term cycling. In order to mitigate the decay in carrying capacity, research has moved towards producing enhanced sorbents. However, this creates potential problems related to ease of scaling up production techniques and production costs, and raises the question as to whether such approaches can be used at large scale. On the other hand, a key advantage of CaL over other carbon capture technologies is synergy with the cement industry, i.e., use of spent sorbent as a feedstock for clinker production. In this work two enhanced materials: (i) limestone doped with HBr through a particle surface impregnation technique; and (ii) pellets prepared from limestone and calcium aluminate cement, were tested in a 25 kW_{th} dual fluidised bed pilot-scale reactor in order to investigate their capture performance and mechanical stability under realistic CaL conditions. Moreover, the spent sorbent was then used as a raw material to make cement, which was characterised for phase and chemical composition as well as compressive strength. The HBr-doped limestone showed better performance in terms of both mechanical strength and stability of the CO_2 uptake when compared to that of pellets. Furthermore, it was shown that the cement produced has similar characteristics and performance as those of commercial CEM 1 cement. This indicates the advantages of using the spent sorbent as feedstock for cement manufacture and shows the benefits of synthetic sorbents in CaL and suitability of end-use of spent sorbents for the cement industry, validating their synergy at pilot scale. Finally, this study demonstrates the possibility of using several practical techniques to improve the performance of CaL at the pilot scale, and more importantly demonstrates that commercial-grade cement can be made from the lime product from this technology.

1. Introduction

CO_2 emissions from the power generation and industrial sectors have increased rapidly in recent decades, and represent the greatest contributors to the greenhouse gas effect [1]. A portfolio of low-carbon technologies needs to be deployed in order to mitigate the effects of these emissions in many natural systems. Carbon capture and storage (CCS) is part of this portfolio and has been proposed as a route for the decarbonisation of power generation and carbon-intensive industrial sectors [2,3].

Calcium looping (CaL) is a second-generation technology for CO_2 capture, which has attracted a fair amount of research activity [4–8]. Typically, a CaL system (Fig. 1) consists of two interconnected fluidised-bed reactors and is based on the reversible carbonation of lime. In the

* Corresponding authors.
E-mail addresses: lyzheng@alum.imr.ac.cn (L. Zheng), b.j.anthony@cranfield.ac.uk (E.J. Anthony).

https://doi.org/10.1016/j.apenergy.2018.05.039
Received 8 March 2018; Received in revised form 24 April 2018; Accepted 6 May 2018

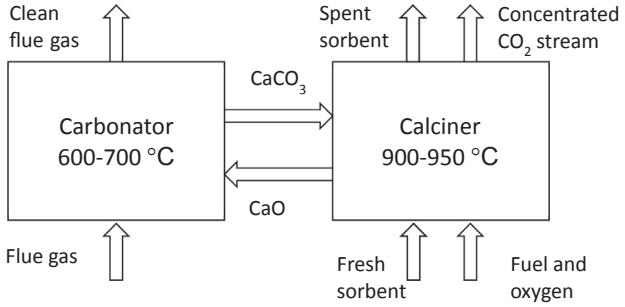

Fig. 1. Schematic of the calcium looping (CaL) cycle.

reactor, operating at ~650 °C (carbonator), CaO-based material is carbonated with the CO_2 present in flue gas or a gas stream from carbon-intensive industrial processes; the saturated sorbent is then transferred to a second reactor operating at ~900 °C (calciner) where the sorbent is regenerated. In order to provide the heat for calcination, a fuel is burnt under oxy-fuel conditions in the calciner, while the high-grade heat generated in the carbonator is intended to be used in a steam cycle.

Due to sorbent deactivation, make-up of fresh and purge of deactivated material are required. One of the unique advantages that the CaL cycle has over other CCS technologies is its synergy with cement production. Namely, it is possible to decarbonise both the cement industry, which is responsible for 7–10% of global anthropogenic CO_2 emissions [9], and the power sector by using the spent sorbent from CO_2 capture as a feedstock for making clinker [6,10–12].

The CaL concept has been demonstrated at scales of up to 1.9 MW_{th} with different reactor configurations. Some examples of these plants include: the 0.1 MW_{th} plant in CanmetENERGY (Ottawa, Canada), the 0.2 MW_{th} pilot plant in IFK (Stuttgart, Germany), the 1.7 MW_{th} unit "La Pereda" run by CSIC in Oviedo, Spain, the 1.9 MW_{th} unit in Taiwan, and the 1 MW_{th} plant in Darmstadt, Germany [13–20].

However, one of the main challenges of this technology, namely the deactivation and loss of active material over the capture/regeneration cycles, still remains [21–23]. The loss of activity is generally attributed to sintering [24–26], attrition and fragmentation [27–29], ash deposition [30], and the competing sulphation reaction [31–33]. In order to overcome this issue, research has focused on the modification of natural materials and the development of synthetic sorbents with techniques such as sol-gel combustion [23,34–38], organic acid modifications [39–43], co-precipitation [44,45], granulation [46–52], and mineral-acid doping [53–55].

Al-Jeboori et al. [53,54] investigated doping of limestone with HBr, HCl, HNO_3 and HI, and the effect on long-term cycling performance of doped sorbents. They demonstrated that such dopants can significantly improve long-term reactivity. The degree of improvement was found to be dependent on the type of limestone used, and the type and concentration of doping agent. The highest residual conversions were observed for Havelock and Longcal limestones doped with HBr (0.167 mol % HBr/$CaCO_3$) [54]. Another effective technique for producing synthetic sorbents for fluidised bed utilisation is the production of calcium aluminate pellets that have been studied at different scales for reactivity and attrition behaviour [47,56]. It has been suggested that the better performance in these synthetic materials is linked to the formation of mayenite ($Ca_{12}Al_{14}O_{33}$), which stabilises the sorbent morphology and mitigates sintering.

This work investigates the capture performance of enhanced CaO sorbents at the pilot scale (25 kW_{th}), under conditions anticipated for real industrial CaL systems. Natural limestone doped with HBr, employing a particle surface impregnation technique, and calcium aluminate pellets were tested in CaL cycles, and the suitability of spent material for use in the cement industry was then explored. The main goal of this study is the pilot demonstration of CaL with enhanced sorbents and its synergy with cement manufacture.

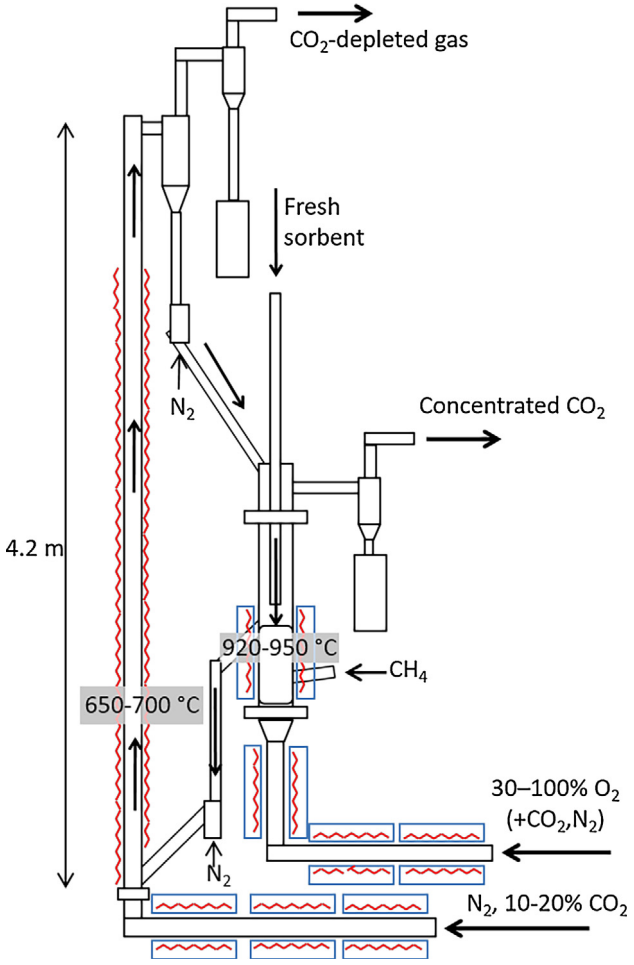

Fig. 2. Schematic of the 25 kWth pilot plant. Note: red lines denote heated sections.

2. Experimental

2.1. Materials

Longcal, a high-purity limestone provided by Longcliffe Ltd, UK, was used as a $CaCO_3$ source. Commercial calcium aluminate cement, CA-14, manufactured by Almatis, was used as a binder in the pelletisation process and as a source of Al_2O_3. The limestone-doping solution was prepared by diluting 57 g of 47%-wt. HBr with deionised water to form 1 L of 0.33 M solution.

2.2. Sorbent preparation procedure

Two types of enhanced sorbents were produced: (i) HBr-doped limestone (0.17 mol% HBr/$CaCO_3$); and (ii) pellets containing 10 wt% calcium aluminate cement and 90 wt% calcined limestone. The pellets were prepared using a Glatt GmbH granulator. A comprehensive description of the pelletisation technique can be found elsewhere [47]. After pelletisation, the particles were sieved to the desired particle size range and air dried for 24 h. HBr was selected as a suitable dopant based on previous work [54]. However, the original doping technique was modified to enable a three-order-of-magnitude increase in production scale. Here, 20 kg of Longcal limestone was evenly sprayed with 1 L of 0.33 M HBr solution, and mixed thoroughly to obtain a uniform distribution of the dopant. The sample was then spread out and dried for several days under ambient conditions.

Table 1
Raw materials used to produce cement clinker.

Cement Clinker	Raw Materials (wt.%)				Spent Sorbent Description
	Spent Sorbent	Clay	SiO_2	Fe_2O_3	
S 1	65.0	25.8	6.2	3.0	SS 1: Spent natural limestone collected from carbonator
S 2	61.7	28.3	6.8	3.2	SS 2: Spent natural limestone collected from calciner
S 3	63.2	27.2	6.5	3.1	SS 3: Spent HBr-doped limestone collected from carbonator
S 4	60.1	29.4	7.1	3.4	SS 4: Spent HBr-doped limestone collected from calciner

2.3. Pilot plant description and operation procedure

The pilot plant (Fig. 2) used in this work consisted of a circulating fluidised bed (CFB) carbonator (4.2 m L and 0.1 m ID) and a bubbling fluidised bed (BFB) calciner (1.2 m L and 0.165 m ID), both operated at atmospheric pressure. The fluidising gases were pre-heated by electrically-heated pipes. The carbonator gas distributor was made up of 8 nozzles (each with 20 2-mm holes) and the calciner gas distributor was made up of 20 nozzles (each with 6 1-mm holes). There were two cyclones in series at the exit of the carbonator. One was used to separate the bulk of the particles in order for them to be recycled to the calciner, and the other was used to prevent the remaining particles from being emitted to the environment. The calciner had a single cyclone. The carbonator and calciner were connected by two loop seals, fluidised by nitrogen, which allowed controlled circulation of sorbent between the reactors. The reactors were electrically heated, and in addition natural gas was oxy-fired directly into the fluidised bed of the calciner to offset the endothermic calcination. Two gas analysers (ADC MGA-3000 series) were used to measure the gas concentrations at the reactor exhausts (CO_2 for the carbonator, and CO_2, CO, O_2, CH_4 for the calciner). Additionally, a Fourier Transform Infrared analyser (FTIR, Protea, model FTPA-002) was used at the exhaust of the calciner to measure H_2O, CO_2, CO, NO_x, SO_2, CH_4, C_2H_6, C_3H_8, C_2H_4, and HCHO concentrations in order to monitor the quality of combustion.

The pilot plant was first heated up to 600 °C by the electrical furnaces surrounding the preheating lines. The first batch of sorbent (3 L) was added to the calciner, which was electrically heated to 650 °C and fluidised by N_2 with superficial velocity 0.35 m/s (mild fluidising conditions). Then, a portion of the N_2 was substituted with O_2 (to reach 40 vol% of O_2) at the inlet of the calciner to combust natural gas with an air-to-fuel equivalence ratio (λ) of 1.05. The bed temperature of the calciner was then ramped up and more sorbent (3 × 1 L) was added when calcination started. A chute, positioned 400 mm above the distributor of the calciner, was used to direct any overflowing material to the lower loop seal and into the carbonator. During the first calcination cycle, the N_2 flow through the carbonator was kept low to prevent backflow into the calciner. After most of the sorbent was calcined (as demonstrated by a sharp temperature increase) the circulation of the material between the reactors was initiated by increasing the N_2 flow in the carbonator (2.5 m/s superficial velocity). The N_2 was used to transport the sorbent from the carbonator to the cyclone where it was separated from the gas and recirculated back to the calciner. Then, the oxygen concentration in the calciner inlet was incrementally increased to 100% to oxy-fire methane. After all the circulating material was calcined, a portion of the inlet gas to the carbonator was substituted with CO_2 (15 vol%) and carbonation was started. The temperature in the calciner during steady-state operation was maintained at 920–950 °C by adjusting the natural gas and O_2 flow rates, and the carbonator temperature was maintained at 650–700 °C. A more detailed description of the experimental procedure can be found elsewhere [57].

It should be noted that the pilot plant operation conditions were chosen to be reasonably close to those anticipated in real applications at commercial scale. However, some additional effects on process performance due to the presence of steam [58], SO_2 [59], and coal ash [30] at industrial scale can be expected, especially if coal, rather than natural gas, is fired in the calciner, owing to its relatively lower price. Under those conditions opposite effects of steam and SO_2 on sorbent conversions can be expected and, in addition to enhanced sorbent sintering, coal ash can cause some additional problems, such as agglomeration, which in extreme cases can lead to defluidisation phenomena.

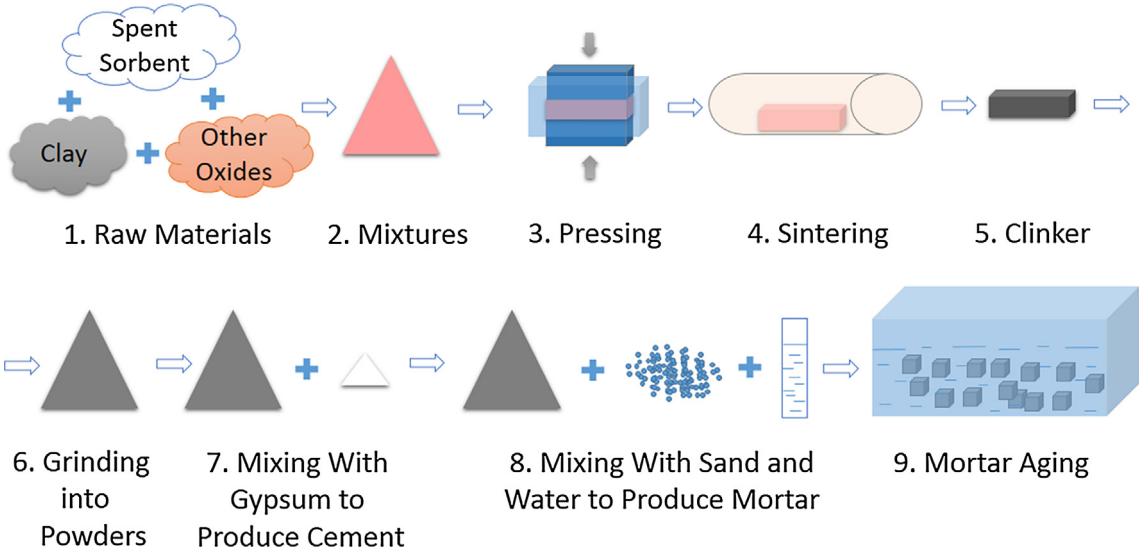

Fig. 3. Schematic diagram of cement production.

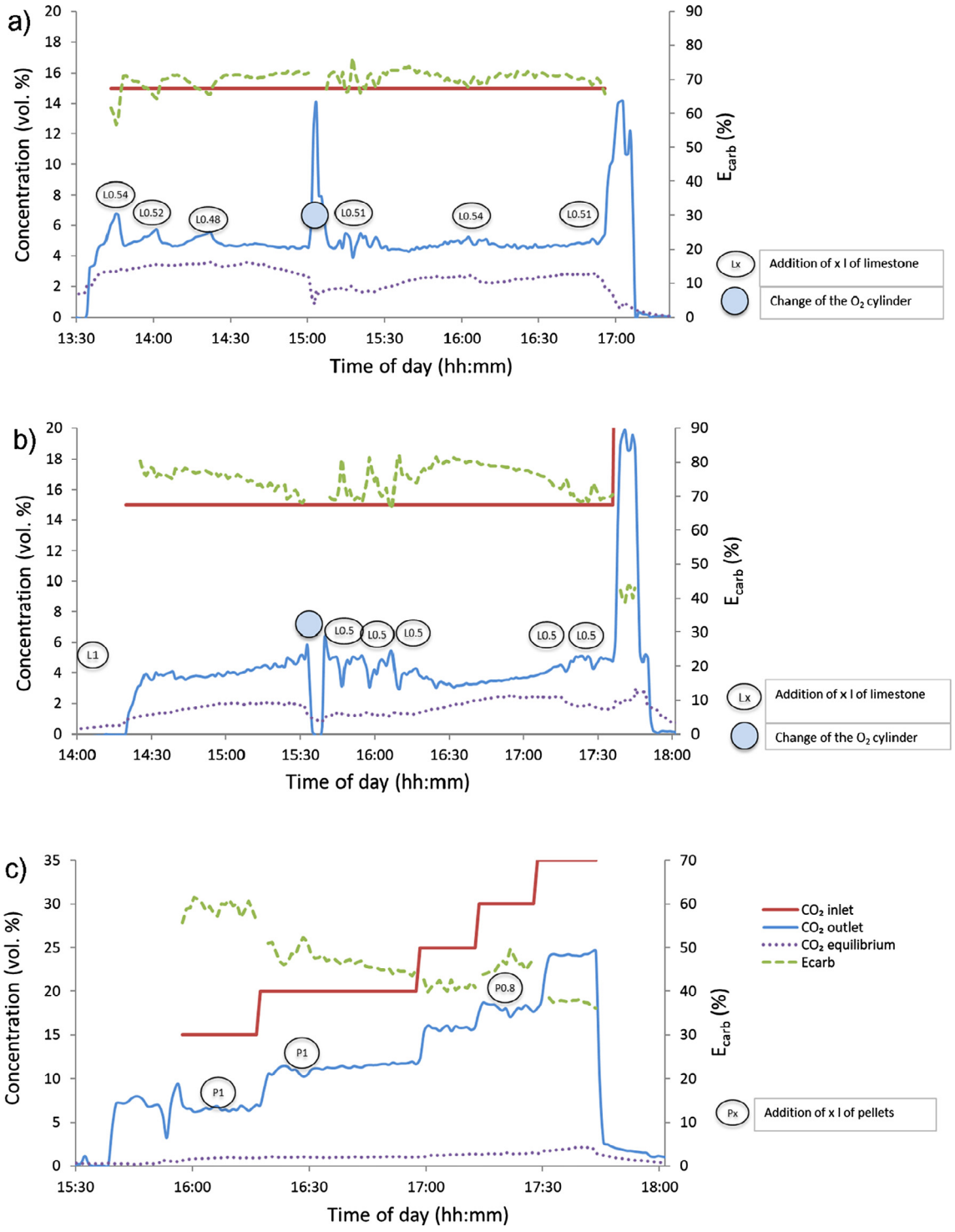

Fig. 4. Concentration of residual CO_2 at the outlet of the carbonator and capture efficiency, E_{carb}, during the pilot plant CaL tests with (a) Longcal limestone, (b) HBr-doped Longcal limestone, and (c) calcium aluminate pellets.

2.4. Cement preparation

Four types of spent sorbent from the pilot-scale tests were used as raw materials to produce cement clinker. SS 1 and SS 2 refer to the spent natural limestone collected from the carbonator and calciner, respectively, and SS 3 and SS 4 refer to the spent HBr-doped limestone collected from the carbonator and calciner, respectively. The corresponding products (clinkers, cements and mortars) were designated as S 1, S 2, S 3, and S 4. For example, SS 1 is spent natural limestone collected from the carbonator, and S 1 designates clinker, cement and mortar produced using SS 1 as a raw material. A summary of the components of each sample is given in Table 1.

Fig. 3 shows a schematic diagram of the cement production process. In order to produce clinker, the spent sorbents were ground into powders and then mixed with commercially-available SiO_2 (< 38 μm) and Fe_2O_3 (< 5 μm) powders, and Bench C clay (< 90 μm) from Southam Quarry, Warks, using a PM-400 (Retsch) planetary ball mill. The mixtures were then pressed into blocks, placed into a platinum boat, and

Table 2
Particle size distribution of Longcal limestone before and after pilot plant CaL test.

Particle Size (μm)	Before	After			
		Carbonator	Carbonator Cyclone	Calciner	Calciner Cyclone
> 355	21%	16%	0%	4%	0%
300–350	43%	45%	1%	38%	1%
250–300	33%	26%	0%	48%	3%
212–250	2%	4%	1%	9%	7%
150–212	0%	3%	14%	1%	35%
63–150	0%	5%	46%	0%	41%
0–63	0%	0%	38%	0%	12%
Total mass (kg)	14.0	1.9	0.12	4.2	2.0

Table 3
Particle size distribution of HBr-doped Longcal limestone before and after pilot plant CaL test.

Particle size (μm)	Before	After			
		Carbonator	Carbonator Cyclone	Calciner	Calciner Cyclone
> 355	13%	5%	3%	4%	17%
300–355	50%	43%	7%	48%	1%
250–300	34%	43%	11%	37%	2%
212–250	1%	7%	3%	9%	4%
150–212	0%	2%	3%	1%	10%
63–150	0%	0%	9%	0%	38%
< 63	0%	0%	64%	0%	28%
Total mass (kg)	13.3	3.1	0.05	4.0	0.37

Table 4
Pore surface area (BET) and elemental analysis (XRF) of HBr-doped Longcal limestone before and after pilot plant CaL test.

	Before	After			
		Carbonator	Carbonator Cyclone	Calciner	Calciner Cyclone
BET (m^2/g)	< 1	1.88	< 1	2.33	1.14
Species (wt.%)					
CaO	99	99	99	99	98
Br	0.29	0.032	0.57	0.025	0.088
MgO	0.26	0.34	0.26	0.33	0.3
SiO_2	0.14	0.17	0.19	0.1	0.37
Al_2O_3	0.11	0.086	0.042	0.061	0.29
SrO	0.036	0.030	0.033	0.030	0.038
MnO	0.019	0.015	0.024	0.015	0.036
SO_3	0.014	ND	0.042	ND	0.14
TiO_2	0.012	0.011	0.011	0.0066	0.021
Fe_2O_3	0.011	0.013	0.095	ND	0.34
Cl	0.005	ND	0.0081	ND	0.006
Cr_2O_3	ND	ND	0.042	ND	0.093
K_2O	ND	ND	0.027	ND	0.016

ND: not detected.

sintered at atmospheric pressure in a horizontal tube furnace (Lenton) at 1500 °C for 1 h under a flowing air atmosphere. After sintering, the blocks were pushed from the centre of the furnace into an air-cooled chamber. Once the samples had cooled down, they were taken out of the furnace and ground into powders. The powders were mixed with 5 wt% gypsum to produce CEM I cement (Portland cement with up to 5% of minor additional constituents) following the BS EN 197-1 standard [60].

2.5. Cement characterisation

The phase compositions of the cement clinkers were identified using an X'Pert Pro (PANalytical) X-ray diffractometer (XRD) using Cu Kα radiation. Quantitative phase analyses were performed using the Rietveld method [61] in the General Structure and Analysis System II (GSAS-II) software [62]. Each phase in the powder pattern was assigned a scale factor based on the unit-cell contents. The Rietveld refinement was used to convert the spectra into quantitative estimates of the weight fractions, with standard uncertainties [62]. The compositions of the cement clinkers were analysed by an Epsilon 3^X X-ray fluorescence (XRF) spectrometer (PANalytical).

A Mastersizer 2000 (Malvern Instruments Ltd) was used to determine the particle size distribution of the cement by laser diffraction. N_2 physisorption was conducted using a Tristar 3000 (Micromeritics) to obtain the Brunauer-Emmett-Teller (BET) surface area of the cement.

Mortar samples were prepared by mixing cement, sand, and water in a weight ratio of 1:1:0.5, respectively. The particle size distribution of the sand was 30% (125–200 μm) + 30% (200–212 μm) + 40% (212–300 μm). The mixture was cast in silicone moulds, shaken (to remove the bubbles), and then placed in a box of water. The samples (with dimensions of approximately 12x12x12 mm) were de-moulded after 24 h, returned to the water, and then tested for compressive strength after 3 d, 7 d, and 28 d using an EZ50 test machine (Lloyd Instruments Ltd) at a compression rate of 100 N/s. Nine cubes were tested for each batch of mortar and the results were compared to the compressive strength of CEMEX CEM I cement (Rugby, UK) reported in our previous work [9].

3. Results and discussion

The results with unmodified Longcal limestone were used as a benchmark in this study. Fig. 4a shows the outlet gas concentration measured by FTIR for a typical experimental run using natural limestone. The corresponding temperature and gas concentration profiles can be found in the ESI† (Fig. SI1). The CO_2 outlet concentration from the carbonator was maintained below 5 vol% by periodic addition of 0.5 L batches of fresh limestone to the calciner. The molar ratio of fresh sorbent make-up to the inlet CO_2 (F_0/F_{CO2}) was 6%, and the make-up ratio (F_0/F_R), where F_R is the molar flow of recycled sorbent inside the loop, was around 1% with an estimated number of carbonation/calcination cycles of 30 per test. These parameters were chosen to maintain the capture efficiency (E_{carb}) around 70% in order to enable comparison of the performance of tested sorbents. Namely, it should be noted that higher make-up ratios would increase capture efficiencies to the near-equilibrium-limited levels and limit comparison of the sorbent performance. After each experiment, the sorbent left in the reactors and in the carbonator and calciner cyclones was collected and its particle size distribution for the base case is provided in Table 2.

3.1. HBr-doped sorbent testing

Compared to the base case with Longcal limestone, using the HBr-doped sorbent improved the CO_2 capture efficiency to 70–80% (Fig. 4b). The corresponding temperature and gas concentration profiles can be found in the ESI† (Fig. SI2). Furthermore, the particle-size-distribution analysis (Table 3) revealed that the doped material exhibited better mechanical properties. Only ~400 g (out of 13 kg in the primary reaction loop) of material was found in the cyclones confirming that there was less attrition compared to the pure limestone case. The shift to a higher particle size distribution range in the calciner cyclone is due to a tendency for the fines to agglomerate, which was not observed in the runs with un-doped Longcal limestone. It should be noted that the particle size distribution differs between the two reactors when using natural limestone. However, this is not the case for the doped limestone. This can be attributed to the lower attrition seen in the doped material.

Table 5
Particle size distribution of calcium aluminate pellets before and after pilot plant CaL test.

Particle size (μm)	Before	After			
		Carbonator	Carbonator Cyclone	Calciner	Calciner Cyclone
> 710	27%	29%	1%	2%	6%
600–710	19%	12%	1%	5%	10%
500–600	19%	12%	2%	10%	14%
425–500	20%	5%	2%	9%	7%
355–425	11%	9%	2%	15%	17%
300–355	3%	14%	8%	27%	9%
250–300	1%	15%	18%	25%	19%
212–250	0%	3%	11%	5%	6%
150–212	0%	1%	17%	1%	4%
63–150	0%	0%	23%	0%	4%
< 63	0%	0%	15%	0%	3%
Total mass (kg)	9.1	3.4	2.6	3.3	1.1

In order to further explore the morphological and composition changes in the sorbent from cycling, XRF and BET analyses of the recovered samples were performed. The results of the XRF analysis (Table 4) suggests that bromine accumulated mainly in the carbonator cyclone fraction. The smallest fraction of the limestone was found in this cyclone (see Table 3), and it can be reasonably hypothesised that bromine is concentrated mainly on the surface of sorbent particles, given the doping technique. This surface is readily attrited during circulation of the particles mainly due to mechanical abrasion generating very small particles [63], which are then collected in the carbonator cyclone. However, the behaviour of the material during the test and the fact that relatively lower overall attrition and breakage of the particles were observed suggest that the doping technique was successful. As the material was found less prone to attrition, there was still a high percentage of Br present in the bed after the test. It is suggested that enhanced performance of the doped sorbent is enabled due to changes in sorbent morphology and stabilisation of its porous structure [64]. Also, it was claimed in our previous work that doping mitigates attrition because the doping agent crystallises in the cracks of the limestone particles making them more resistant to mechanical stresses [63]. Finally, the doping method proposed in this study potentially uses less HBr (per mass of limestone) than the lab-scale wet impregnation technique reported previously [54], and is a more cost-effective approach for industrial-scale doping.

The economic analysis of sorbent treatment is one of the key parameters to estimate if the CaL process with doped sorbent would be viable. The doping technique proposed in this study is not complex, and the major increase in sorbent cost would be due to the cost of HBr. Assuming that the cost of hydrobromic acid (48 wt%) is ~$1000/t [65] and the cost of limestone is ~$15/t [66], it can be estimated that the cost of the doped material would be about $18/t, which is a 20% increase in the cost of sorbent. It was recently demonstrated that changes in sorbent cost of this magnitude have a negligible effect on the levelised cost of electricity (LCOE) and cost of CO_2 avoided [67]. For comparison, in the case of the benchmark technology for carbon capture (amine scrubbing) the solvent cost is $1000/t [68]; therefore, even if the doping technique increases the price of the sorbent by a magnitude of 20%, the cost of the doped sorbent is still significantly lower than the cost of the amine solvent.

3.2. Calcium aluminate pellets testing

The temperature and gas concentration profiles for CaL tests using calcium aluminate pellets are given in the ESI† (Fig. SI3). The capture efficiency (Fig. 4c) was found to be substantially lower than that for the base case and the HBr-doped limestone case. The main limitation with this case was the amount of available adsorbent for capturing CO_2 due to attrition. A possible solution would be to increase the carbonator height to achieve longer residence times. As shown in Table 5, it is clear that some of the pellets were fragmented or attrited but the bulk of them were retained within the CaL rig. However, their performance was not as good as that of the other sorbents, and there were some difficulties related to their use. These included excessive release of steam during the rapid heating stage, which can be solved by using pre-calcined material. Moreover, the results of the XRF and BET analyses can be found in Table 6. The results presented in this work are in accordance with those obtained by Symonds et al. [13] with regard to the use of calcium aluminate pellets; their performance appears worse than the performance of natural limestone. Moreover, there are certain operating difficulties found when these particles are used as a CaL sorbent at larger scale.

Table 6
Pore surface area (BET) and elemental analysis (XRF) of calcium aluminate pellets before and after pilot plant CaL test.

	Before	After			
		Carbonator	Carbonator Cyclone	Calciner	Calciner Cyclone
BET (m^2/g)	19	3	4.2	3.1	3.6
Species (wt.%)					
CaO	93	94	96	95	97
Br	ND	0.057	0.056	0.043	0.10
MgO	0.27	0.30	0.30	0.32	0.28
SiO_2	0.13	0.22	0.15	0.1	0.17
Al_2O_3	6.9	5.4	2.9	4.5	2.1
SrO	0.03	0.029	0.032	0.032	0.032
MnO	0.020	0.016	0.017	0.016	0.017
SO_3	0.012	ND	0.019	0.012	0.016
TiO_2	0.031	ND	0.007	0.009	0.018
Fe_2O_3	0.026	0.015	0.033	0.016	0.035
Cl	ND	0.007	0.006	0.009	ND
Cr_2O_3	ND	ND	ND	ND	ND
K_2O	0.008	ND	ND	ND	0.015

ND: not detected.

One potential advantage of using pellets is attributed to the potential for producing them from spent sorbents since pelletisation has been demonstrated as a reactivation strategy [69]. Furthermore, the conversion of the pellets can be improved by pre-carbonation [70]. This can be potentially carried out by capturing residual CO_2 from low-emitting sources, such as the low-CO_2-concentration stream leaving the carbonator. Ridha et al. [71] have shown that it was possible to achieve this at ambient temperatures. This would not only improve the performance of synthetic materials in real systems owing to less mechanical stress within the particle from steam release, but would also help improve the overall capture efficiency of these plants.

3.3. Cement chemical compositions

After the pilot-scale testing, the spent sorbent was recovered and used to form clinker. XRD patterns of the spent sorbents can be found in the ESI† (Fig. SI4). Two phases ($CaCO_3$ and CaO) were detected in the spent sorbents SS 1, SS 2, SS 3, and SS 4.

3.3.1. Clinker phase compositions

In order to obtain high-quality cement, it is necessary to control the phase distribution of its four major components: Alite Ca_3SiO_5 (C_3S in cement notation), Belite Ca_2SiO_4 (C_2S), the aluminate phase $Ca_3Al_2O_6$ (C_3A) and the ferrite phase $Ca_4(Al, Fe)_4O_{10}$ (C_4AF). Fig. 5 shows the XRD patterns of the cement clinkers produced using different spent sorbents in air at 1500 °C for 1 h. It can be seen that all the clinkers possessed similar XRD patterns and, therefore, the same phases. These

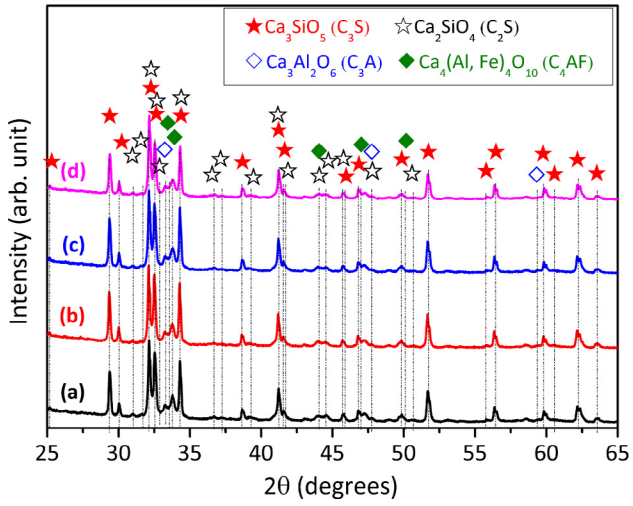

Fig. 5. X-ray diffraction (XRD) patterns of cement clinkers produced using spent sorbents in air at 1500 °C for 1 h: (a) S 1, (b) S 2, (c) S 3, (d) S 4.

four phases react at different rates with water and, therefore, contribute differently to the overall performance of the cement. For example, Alite reacts relatively quickly, and is the most important constituent in normal Portland cements for strength development at ages up to 28 d. On the other hand, Belite reacts slowly, and thus contributes little to the strength during the first 28 d. However, Belite can substantially increase the strength of cement at later stages [72]. In CEM I, Alite, Belite, the aluminate phase and ferrite phase constitute 50–70%, 15–30%, 5–10% and 5–15% of the clinkers, respectively [72].

Quantitative phase analysis of the produced cement clinkers was conducted using GSAS-II data analysis software. During the refinement in GSAS-II, Ca_3SiO_5 (monoclinic, *Cm* (8)), Ca_2SiO_4 (monoclinic, $P2_1/n$ (14)), $Ca_3Al_2O_6$ (cubic, *Pa*-3 (205)) and $Ca_4(Al, Fe)_4O_{10}$ (orthorhombic, *Ibm*2 (46)) were used as the import phases and the experimental patterns were obtained using XRD. Fig. 6 illustrates the profile fit and difference patterns of the clinkers using GSAS-II. The red solid line is the calculated pattern, the black crosses overlying it are the experimental pattern, and the blue line at the bottom represents the difference between the two. The four sets of vertical dashes below the spectra mark the peak positions of C_3S, C_2S, C_3A and C_4AF according to their Bragg reflections, respectively. It can be seen that the calculated pattern and the experimental pattern match well with each other for all the produced cement clinkers. The differential curve is smooth, suggesting successful refinement. R_{wp} (Rietveld weighted-profile R-factor) and GOF (goodness of fit) values of the final refinements are also given in each graph. These values suggest that the Rietveld fits were of high quality. A more detailed description on how to judge the quality of the Rietveld fits has been illustrated in our previous work [9] and elsewhere [73,74]. The quantitative data on the phase compositions of the produced cement clinkers obtained using Rietveld refinement in GSAS-II are shown in Fig. 7. It can be seen that all the produced clinkers are similar to the CEM I clinker in phase compositions (see Table 7).

3.3.2. Oxide compositions

The oxide compositions of the produced clinkers as measured by XRF are given in Table 7. The results demonstrate that the compositions all fall within the same range of oxide compositions for CEM I clinker. Oxide compositions were calculated using the phase compositions obtained by GSAS II, according to Eqs. (1)–(4):

$$CaO = 0.7368*C_3S + 0.6512*C_2S + 0.6222*C_3A + 0.4609*C_4AF \quad (1)$$

$$SiO_2 = 0.2632*C_3S + 0.3488*C_2S \quad (2)$$

$$Al_2O_3 = 0.3778*C_3A + 0.2099*C_4AF \quad (3)$$

$$Fe_2O_3 = 0.3292*C_4AF \quad (4)$$

The above calculations were based on the assumptions that all the four main phases, C_3S, C_2S, C_3A and C_4AF, existed as pure phases. The calculated results were consistent with those measured by XRF.

The fact that the chemical and oxide compositions of the produced clinkers match those of CEM 1 supports the contention that the spent sorbents derived from CaL with unmodified and doped limestones are suitable for cement clinker production.

3.4. Fineness

The fineness of cement has an important effect on the compressive strength development because it affects its hydration rate. When exposed to water, phases in the cement start to react, and a layer of hydrated product forms around the outside of the particle. This layer separates the unreacted core of the particle from the surrounding water and as this layer grows thicker, the rate of hydration slows down [75]. Particle size distribution and BET surface area are two effective parameters that can be used to describe the fineness of the cement.

Table 8 shows the particle size distribution of the produced cements using different spent sorbents compared to that of the commercially available CEMEX CEM I. Cements S 2 and S 3 were found to have similar particle size distributions to that of CEMEX CEM I; while cements S 1 and S 4 had a greater portion of larger particles. It can be seen that the median particle size by volume, d (0.5) of S 1, S 2, S 3, S 4 and CEMEX CEM I are 21.1 μm, 14.6 μm, 13.6 μm, 24.9 μm and 15.8 μm, respectively. Additionally, BET surface areas of the produced different cements, S 1, S 2, S 3, S 4 were measured to be 1.61 m^2/g, 1.91 m^2/g, 2.19 m^2/g, and 1.23 m^2/g, respectively. The small differences on the particle size distributions and BET surface areas of the produced different cements are reasonable and within the procedural experimental error. These results suggest that the fineness of the cements prepared is suitable for CEM 1.

3.5. Compressive strength

Fig. 8 shows the compressive strength of each cement compared with the CEMEX CEM I from 3 days up to 28 d. The results suggest that the compressive strengths of the produced cements are comparable with those of the commercially-available cement at each testing age. There were no significant differences among the compressive strengths of the cements produced using the different spent sorbents as raw materials. It can be seen that the compressive strengths of the cements increase with age, as expected. For example, the compressive strength of cement S 2 increased from 41.0 MPa to 51.9 MPa from its 7-d to its 28-d test. The individual plots of compressive strengths can be found in the ESI† (Fig. SI5).

3.6. End use of lime-based sorbents

The potential sinks for lime-based materials in the cement industry have been analysed in detail in a recent book on Ca and Chemical Looping [8]. If we take an approximate global figure for coal-fired plant of about 8000 TWh [76], simple calculations will show that this is equivalent to 1100 Mt/a of cement manufacture, which is less than the 3800 Mt/a required for cement production for cement manufacture worldwide [77], and in the case of countries such as India and China the demand for cement is considerably greater than all the product produced if their coal-fired units were converted to CaL and the product used for cement manufacture.

4. Conclusions

The use of enhanced materials for CaL was studied at pilot scale in this work. A modified technique for impregnating the surface of

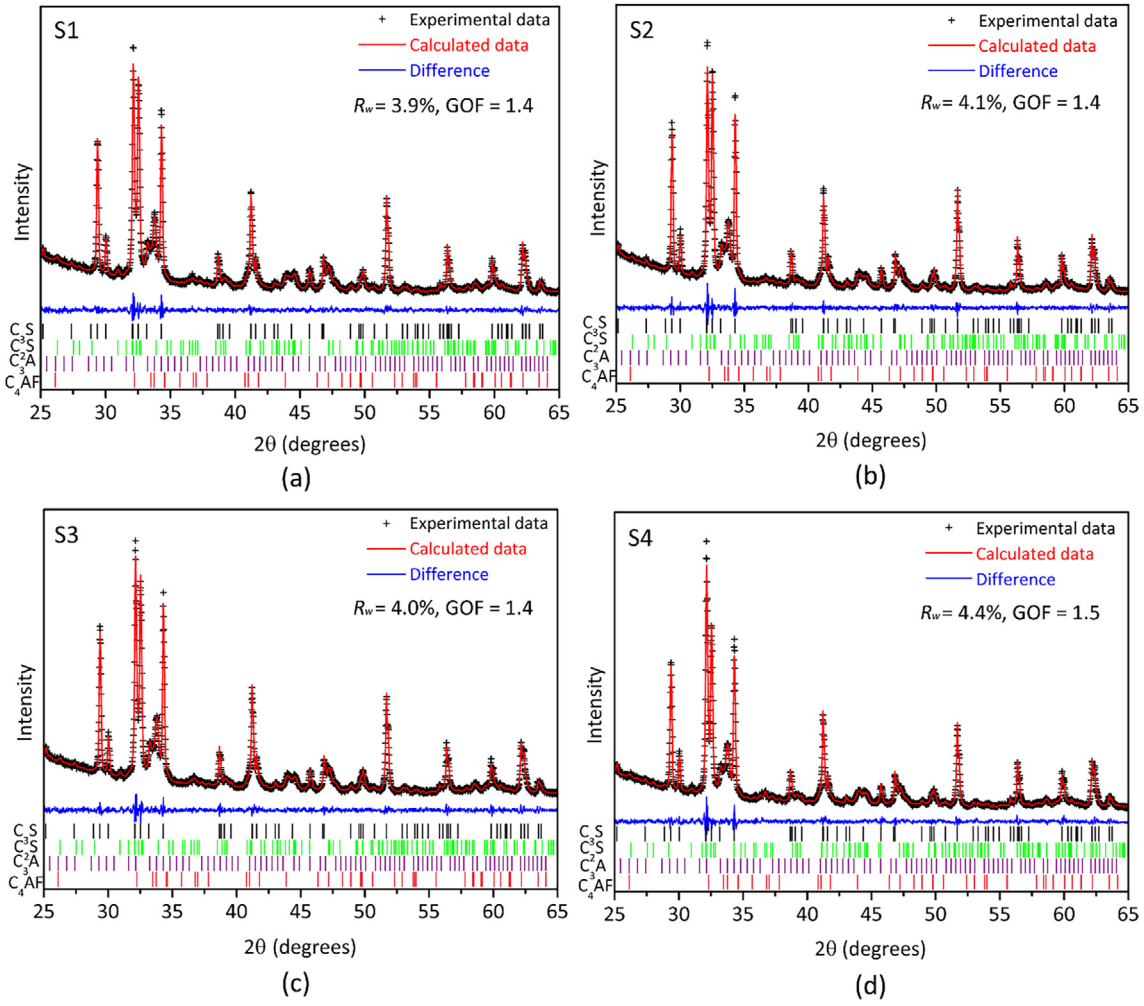

Fig. 6. Rietveld Refinement (GSAS II) patterns of cement clinkers produced using spent sorbents in air at 1500 °C for 1 h: (a) S 1, (b) S 2, (c) S 3, (d) S 4.

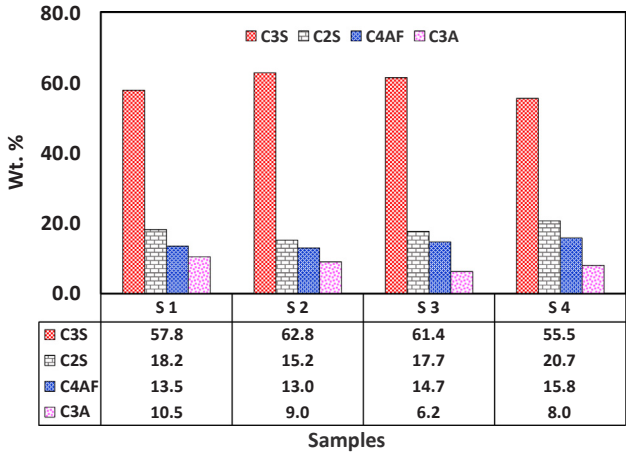

Fig. 7. Phase compositions, as calculated by Rietveld refinement of the XRD data, of cement clinkers produced using spent sorbents in air at 1500 °C for 1 h.

limestone with HBr is described here and both the doped sorbents and calcium aluminate pellets were tested in the pilot CaL system. The HBr-doped material showed enhanced mechanical stability and better capture performance than the untreated limestone, with capture efficiency 70–80% at a relatively low make-up ratio (1%) during stable steady operation. It should be noted that the surface of the particle was modified by the enhancement technique and hence as the particles attrited, most of the bromine was found to accumulate in the carbonator cyclone. However, the start-up procedure with calcium aluminate pellets was more challenging, especially due to the release of steam when calcining that material in the fluidised bed. However, this can be avoided by exposing the pelletised material to low-concentration CO_2 sources, e.g., the exhaust gas coming from the carbonator (~2% residual CO_2) in order to pre-carbonate calcium hydroxide in the pellets, which would result in a higher overall capture efficiency. This also can potentially increase the mechanical stability of the pellets, which needs to be further improved.

Cement clinkers were successfully produced using different spent sorbents from the pilot CaL CO_2 capture tests. The phase and oxide compositions of the produced cement clinkers were obtained by XRD and XRF measurements, as well as quantitative phase analysis using GSAS II. The results show that all the produced cement clinkers have similar compositions to CEM I clinker. The compressive strength of mortars prepared from the clinkers was in the range of that for mortar prepared from commercially-available CEMEX CEM I.

The results from pilot plant tests presented in this study clearly confirm the viability of using modified sorbents, such as HBr-doped limestone, in CaL systems, and that the spent materials can be used as raw materials to produce cements. Also, this study demonstrated at pilot scale the synergy of CaL and the cement industry, recommending the CaL cycle as an obvious technology choice for decarbonisation of that carbon-intensive industry.

Table 7
Oxide compositions of the produced clinker as measured by XRF and calculated using GSAS II results.

Cement Clinker	Method	Oxides Compositions (wt.%)									
		CaO	SiO_2	Al_2O_3	Fe_2O_3	MgO	K_2O	Na_2O	SO_3	TiO_2	Others
S 1	XRF	65.8	18.9	4.8	6.9	0.8 3.6	0.8	0.2	1.3	0.2	0.3
	GSAS II	67.2	21.6	6.8	4.4						
S 2	XRF	66.3	18.8	4.7	6.7	0.8 3.5	0.7	0.2	1.3	0.2	0.3
	GSAS II	67.8	21.8	6.1	4.3						
S 3	XRF	66.2	19.0	4.8	6.4	0.8 3.6	0.7	0.2	1.4	0.2	0.3
	GSAS II	67.4	22.3	5.4	4.8						
S 4	XRF	66.5	18.4	4.5	6.4	0.7 4.2	0.9	0.2	1.8	0.2	0.4
	GSAS II	66.6	21.8	6.3	5.2						
CEM I		~67	~22	~5	~3	< 3					

Table 8
Particle size distribution and BET surface area of the produced cements and CEMEX CEM I.

Cement	d (0.1) (μm)	d (0.5) (μm)	d (0.9) (μm)	Vol.% (0–30 μm)	Vol.% (0–45 μm)	Vol.% (0–60 μm)	BET Surface Area (m^2/g)
S 1	3.9	21.1	62.5	64.1	80.1	89.0	1.61
S 2	2.9	14.6	38.6	81.9	94.0	98.2	1.91
S 3	2.5	13.6	36.4	83.9	95.4	99.2	2.19
S 4	5.1	24.9	63.1	58.7	77.8	88.5	1.23
CEMEX CEM I	3.5	15.8	39.8	79.8	93.5	98.1	n/a

d (0.1), d (0.5), and d (0.9) represent 10%, 50% and 90% of the volume distribution are below these value, respectively.

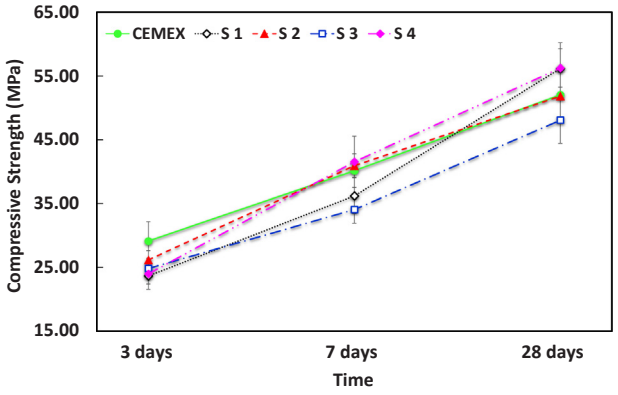

Fig. 8. Compressive strength development of the produced mortars upon aging.

Acknowledgements

The authors wish to thank Mr. Martin Roskilly and Mr Howard Smith for their support and advice during this investigation. The research leading to these results has received funding from the European Community's Research Fund for Coal and Steel (RFCS) under grant agreement no. RFCR-CT-2014-00007. This work was funded by the UK Carbon Capture and Storage Research Centre (UKCCSRC) as part of Call 2 projects. UKCCSRC is supported by the Engineering and Physical Sciences Research Council (EPSRC) as part of the Research Council's UK Energy Programme, with additional funding from the Department of Business, Energy and Industrial Strategy (BEIS – formerly DECC). In addition, the authors wish to thank Almantis Inc. and Longcliffe UK for providing the materials used in this work. Requests for cement preparation data should be sent to https://www.imperial.ac.uk/people/p.fennell. Data underlying the pilot plant testing depicted in this paper can be accessed at https://doi.org/10.17862/cranfield.rd.6255758.

Appendix A. Supplementary material

Supplementary data associated with this article can be found, in the online version, at http://dx.doi.org/10.1016/j.apenergy.2018.05.039.

References

[1] IPCC. Climate change 2014: synthesis report. Contribution of Working Groups I, II and III to the fifth assessment report of the intergovernmental panel on climate change, Geneva, Switzerland; 2014.
[2] Bernstein L, Lee A, Crookshank S. Carbon dioxide capture and storage: a status report; 2006.
[3] Boot-Handford ME, Abanades JC, Anthony EJ, Blunt MJ, Brandani S, Mac Dowell N, et al. Carbon capture and storage update. Energy Environ Sci 2014;7(1):130–89.
[4] Erans M, Manovic V, Anthony EJ. Calcium looping sorbents for CO_2 capture. Appl Energy 2016;180:722–42.
[5] Blamey J, Anthony EJ, Wang J, Fennell PS. The calcium looping cycle for large-scale CO_2 capture. Prog Energy Combust Sci 2010;36(2):260–79.
[6] Dean CC, Blamey J, Florin NH, Al-Jeboori MJ, Fennell PS. The calcium looping cycle for CO_2 capture from power generation, cement manufacture and hydrogen production. Chem Eng Res Des 2011;89(6):836–55.
[7] Dean CC, Dugwell D, Fennell PS. Investigation into potential synergy between power generation, cement manufacture and CO_2 abatement using the calcium looping cycle. Energy Environ Sci 2011;4(6):2050–3.
[8] Fennell PS, Anthony EJ. Calcium and chemical looping technology for power generation and carbon dioxide (CO2) capture. Woodhead Publishing Series in Energy; 2015.
[9] Zheng L, Hills TP, Fennell P. Phase evolution, characterisation, and performance of cement prepared in an oxy-fuel atmosphere. Faraday Discuss 2016;192:113–24.
[10] Arias B, Alonso M, Abanades C. CO_2 capture by calcium looping at relevant conditions for cement plants: experimental testing in a 30 kW_{th} pilot plant. Ind Eng Chem Res 2017;56(10):2634–40.
[11] Romano MC, Spinelli M, Campanari S, Consonni S, Cinti G, Marchi M, et al. The Calcium looping process for low CO_2 emission cement and power. Energy Procedia 2013;37:7091–9.
[12] Telesca A, Calabrese D, Marroccoli M, Tomasulo M, Valenti GL, Duelli G, et al. Spent limestone sorbent from calcium looping cycle as a raw material for the cement industry. Fuel 2014;118:202–5.
[13] Symonds RT, Champagne S, Ridha FN, Lu DY. CO_2 capture performance of CaO–based pellets in a 0.1 MW_{th} pilot-scale calcium looping system. Powder Technol 2016;290:124–31.
[14] Hawthorne C, Dieter H, Bidwe A, Schuster A, Scheffknecht G, Unterberger S, et al.

CO_2 capture with CaO in a 200 kW_{th} dual fluidized bed pilot plant. Energy Procedia 2011;4:441–8.
[15] Sánchez-Biezma A, Ballesteros JC, Diaz L, De Zárraga E, Álvarez FJ, López J, et al. Postcombustion CO_2 capture with CaO. Status of the technology and next steps towards large scale demonstration. Energy Procedia 2011;4:852–9.
[16] Dieter H, Hawthorne C, Zieba M, Scheffknecht G. Progress in calcium looping post combustion CO_2 capture: successful pilot scale demonstration. Energy Procedia 2013;37:48–56.
[17] Arias B, Diego ME, Abanades JC, Lorenzo M, Diaz L, Martínez D, et al. Demonstration of steady state CO_2 capture in a 1.7 MW_{th} calcium looping pilot. Int J Greenhouse Gas Control 2013;18:237–45.
[18] Ströhle J, Junk M, Kremer J, Galloy A, Epple B. Carbonate looping experiments in a 1 MW_{th} pilot plant and model validation. Fuel 2014;127:13–22.
[19] Bidwe AR, Hawthorne C, Dieter H, Dominguez MA, Zieba M, Scheffknecht G. Cold model hydrodynamic studies of a 200 kW_{th} dual fluidized bed pilot plant of calcium looping process for CO_2 capture. Powder Technol 2014;253:116–28.
[20] Chang MH, Chen WC, Huang CM, Liu WH, Chou YC, Chang WC, et al. Design and experimental testing of a 1.9 MW_{th} calcium looping pilot plant. Energy Procedia 2014;63:2100–8.
[21] Chen Z, Song HS, Portillo M, Lim CJ, Grace JR, Anthony EJ. Long-term calcination/carbonation cycling and thermal pretreatment for CO_2 capture by limestone and dolomite. Energy Fuels 2009;23(3):1437–44.
[22] Fennell PS, Pacciani R, Dennis JS, Davidson JF, Hayhurst AN. The effects of repeated cycles of calcination and carbonation on a variety of different limestones, as measured in a hot fluidized bed of sand. Energy Fuels 2007;21(4):2072–81.
[23] Grasa GS, Abanades JC. CO_2 capture capacity of CaO in long series of carbonation/calcination cycles. Ind Eng Chem Res 2006;45(26):8846–51.
[24] Borgwardt RH. Sintering of nascent calcium oxide. Chem Eng Sci 1989;44(1):53–60.
[25] Borgwardt RH. Calcium oxide sintering in atmospheres containing water and carbon dioxide. Ind Eng Chem Res 1989;28(4):493–500.
[26] Sun P, Grace JR, Lim CJ, Anthony EJ. The effect of CaO sintering on cyclic CO_2 capture in energy systems. AIChE J 2007;53(9):2432–42.
[27] Coppola A, Montagnaro F, Salatino P, Scala F. Attrition of limestone during fluidized bed calcium looping cycles for CO_2 capture. Combust Sci Technol 2012;184(7–8):929–41.
[28] González B, Alonso M, Abanades JC. Sorbent attrition in a carbonation/calcination pilot plant for capturing CO_2 from flue gases. Fuel 2010;89(10):2918–24.
[29] Scala F, Salatino P. Limestone fragmentation and attrition during fluidized bed oxyfiring. Fuel 2010;89(4):827–32.
[30] He D, Qin C, Manovic V, Ran J, Feng B. Study on the interaction between CaO-based sorbents and coal ash in calcium looping process. Fuel Process Technol 2017;156:339–47.
[31] Coppola A, Montagnaro F, Salatino P, Scala F. Fluidized bed calcium looping: the effect of SO_2 on sorbent attrition and CO_2 capture capacity. Chem Eng J 2012;207:445–9.
[32] Scala F, Cammarota A, Chirone R, Salatino P. Comminution of limestone during batch fluidized-bed calcination and sulfation. AIChE J 1997;43(2):363–73.
[33] Stanmore BR, Gilot P. Calcination and carbonation of limestone during thermal cycling for CO_2 sequestration. Fuel Process Technol 2005;86(16):1707–43.
[34] Luo C, Zheng Y, Ding N, Wu Q, Bian G, Zheng C. Development and performance of CaO/La_2O_3 sorbents during calcium looping cycles for CO_2 capture. Ind Eng Chem Res 2010;49(22):11778–84.
[35] Luo C, Zheng Y, Zheng C, Yin J, Qin C, Feng B. Manufacture of calcium-based sorbents for high temperature cyclic CO_2 capture via a sol–gel process. Int J Greenhouse Gas Control 2013;12:193–9.
[36] Radfarnia HR, Sayari A. A highly efficient CaO-based CO_2 sorbent prepared by a citrate-assisted sol–gel technique. Chem Eng J 2015;262:913–20.
[37] Wang B, Yan R, Lee DH, Zheng Y, Zhao H, Zheng C. Characterization and evaluation of Fe_2O_3/Al_2O_3 oxygen carrier prepared by sol–gel combustion synthesis. J Anal Appl Pyrol 2011;91(1):105–13.
[38] Broda M, Müller CR. Sol–gel-derived, CaO-based, ZrO_2-stabilized CO_2 sorbents. Fuel 2014;127:94–100.
[39] Zhang M, Peng Y, Sun Y, Li P, Yu J. Preparation of CaO–Al_2O_3 sorbent and CO_2 capture performance at high temperature. Fuel 2013;111:636–42.
[40] Li Y, Su M, Xie X, Wu S, Liu C. CO_2 capture performance of synthetic sorbent prepared from carbide slag and aluminum nitrate hydrate by combustion synthesis. Appl Energy 2015;145:60–8.
[41] Li CC, Wu UT, Lin HP. Cyclic performance of $CaCO_3$@ $mSiO_2$ for CO_2 capture in a calcium looping cycle. J Mater Chem A 2014;2(22):8252–7.
[42] Li L, King DL, Nie Z, Howard C. Magnesia-stabilized calcium oxide absorbents with improved durability for high temperature CO_2 capture. Ind Eng Chem Res 2009;48(23):10604–13.
[43] Zhao M, Bilton M, Brown AP, Cunliffe AM, Dvininov E, Dupont V, et al. Durability of CaO–$CaZrO_3$ sorbents for high-temperature CO_2 capture prepared by a wet chemical method. Energy Fuels 2014;28(2):1275–83.
[44] Gupta H, Fan LS. Carbonation− calcination cycle using high reactivity calcium oxide for carbon dioxide separation from flue gas. Ind Eng Chem Res 2002;41(16):4035–42.
[45] Florin N, Fennell PS. Synthetic CaO-based sorbent for CO_2 capture. Energy Procedia 2011;4:830–8.
[46] Manovic V, Anthony EJ. Screening of binders for pelletization of CaO-based sorbents for CO_2 capture. Energy Fuels 2009;23(10):4797–804.
[47] Wu Y, Manovic V, He I, Anthony EJ. Modified lime-based pellet sorbents for high-temperature CO_2 capture: reactivity and attrition behavior. Fuel 2012;96:454–61.
[48] Ridha FN, Manovic V, Macchi A, Anthony EJ. High-temperature CO_2 capture cycles for CaO-based pellets with kaolin-based binders. Int J Greenhouse Gas Control 2012;6:164–70.
[49] Qin C, Yin J, An H, Liu W, Feng B. Performance of extruded particles from calcium hydroxide and cement for CO_2 capture. Energy Fuels 2011;26(1):154–61.
[50] Ridha FN, Wu Y, Manovic V, Macchi A, Anthony EJ. Enhanced CO_2 capture by biomass-templated $Ca(OH)_2$-based pellets. Chem Eng J 2015;274:69–75.
[51] Manovic V, Anthony EJ. CaO-based pellets with oxygen carriers and catalysts. Energy Fuels 2011;25(10):4846–53.
[52] Erans M, Beisheim T, Manovic V, Jeremias M, Patchigolla K, Dieter H, et al. Effect of SO_2 and steam on CO_2 capture performance of biomass-templated calcium aluminate pellets. Faraday Discuss 2016;192:97–111.
[53] Al-Jeboori MJ, Fennell PS, Nguyen M, Feng K. Effects of different dopants and doping procedures on the reactivity of CaO-based sorbents for CO_2 capture. Energy Fuels 2012;26(11):6584–94.
[54] Al-Jeboori MJ, Nguyen M, Dean C, Fennell PS. Improvement of limestone-based CO_2 sorbents for Ca looping by HBr and other mineral acids. Ind Eng Chem Res 2013;52(4):1426–33.
[55] González B, Blamey J, Al-Jeboori MJ, Florin NH, Clough PT, Fennell PS. Additive effects of steam addition and HBr doping for CaO-based sorbents for CO_2 capture. Chem Eng Process Process Intensif 2016;103:21–6.
[56] Manovic V, Anthony EJ. Long-term behavior of CaO-based pellets supported by calcium aluminate cements in a long series of CO_2 capture cycles. Ind Eng Chem Res 2009;48(19):8906–12.
[57] Erans M, Jeremiáš M, Manovic V, Anthony EJ. Operation of a 25 kWth calcium looping pilot-plant with high oxygen concentration in the calciner. JoVe 2017;2017(128):e56112.
[58] Manovic V, Fennell PS, Al-Jeboori MJ, Anthony EJ. Steam-enhanced calcium looping cycles with calcium aluminate pellets doped with bromides. Ind Eng Chem Res 2013;52(23):7677–83.
[59] Ridha FN, Manovic V, Macchi A, Anthony EJ. The effect of SO_2 on CO_2 capture by CaO-based pellets prepared with a kaolin derived $Al(OH)_3$ binder. Appl Energy 2012;92:415–20.
[60] European Committee for Standardization. European Standard EN 197-1; 2000.
[61] Rietveld H. A profile refinement method for nuclear and magnetic structures. J Appl Crystallogr 1969;2(2):65–71.
[62] Toby BH, Von Dreele RB. GSAS-II: the genesis of a modern open-source all-purpose crystallography software package. J Appl Crystallogr 2013;46(2):544–9.
[63] Scala F. Fluidized bed technologies for near-zero emission combustion and gasification. Elsevier; 2013.
[64] González B, Blamey J, McBride-Wright M, Carter N, Dugwell D, Fennell P, et al. Calcium looping for CO_2 capture: sorbent enhancement through doping. Energy Procedia 2011;4:402–9.
[65] Alibaba. https://www.alibaba.com/product-detail/High-Purity-48-HBr-Hydrobromic-Acid_60707033707.html?spm=a2700.7724857.main07.131.59aa1624r7XJFr [accessed 25/01/2018].
[66] Rubin ES, Kalagnanam JR, Frey HC, Berkenpas MB. Integrated environmental control modelling of coal-fired power systems. J Air Waste Manag Assoc 1997;47(11):1180–8.
[67] Hanak DP, Manovic V. Economic feasibility of calcium looping under uncertainty. Appl Energy 2017;208:691–702.
[68] Romeo LM, Bolea I, Escosa JM. Integration of power plant and amine scrubbing to reduce CO_2 capture costs. Appl Therm Eng 2008;28(8–9):1039–46.
[69] Manovic V, Wu Y, He I, Anthony EJ. Spray water reactivation/pelletization of spent CaO-based sorbent from calcium looping cycles. Environ Sci Technol 2012;46(22):12720–5.
[70] Materić V, Edwards S, Smedley SI, Holt R. $Ca(OH)_2$ superheating as a low-attrition steam reactivation method for CaO in calcium looping applications. Ind Eng Chem Res 2010;49(24):12429–34.
[71] Ridha FN, Manovic V, Macchi A, Anthony EJ. CO_2 capture at ambient temperature in a fixed bed with CaO-based sorbents. Appl Energy 2015;140:297–303.
[72] Taylor HF. Cement chemistry. London: Academic Press; 1990.
[73] Toby BH. R factors in Rietveld analysis: how good is good enough? Powder Diffract 2006;21(1):67–70.
[74] McCusker LB, Von Dreele RB, Cox DE, Louër D, Scardi P. Rietveld refinement guidelines. J Appl Crystallogr 1999;32(1):36–50.
[75] Thomas J, Jennings H. The science of concrete. http://iti.northwestern.edu/cement/index.html [accessed 28/06/2017].
[76] Yang A, Cui Y. Global coal risk assessment: data analysis and market research [Working Paper]. World Resources Institute; 2012.
[77] U.S. Geological Survey. Mineral commodity summaries 2014. USGS 2014:38–9.